

Original Research Article

Green synthesis of silver nanoparticles using *Arbutus andrachne* leaf extract and its antimicrobial activity

Tuğçe Erdoğan¹, Fethiye Ferda Yılmaz², Bijen Kivçak¹ and Mine Özyazıcı^{3*}

¹Department of Pharmacognosy, ²Department of Pharmaceutical Microbiology, ³Department of Pharmaceutical Technology, Faculty of Pharmacy, Ege University, Bornova, Izmir, Turkey

*For correspondence: **Email:** mine.ozyazici@ege.edu.tr; **Tel:** +90 232 3111357; **Fax:** +90 232 3885258

Received: 13 February 2015

Revised accepted: 16 April 2016

Abstract

Purpose: To synthesize silver nanoparticles (AgNPs) of *Arbutus andrachne* leaf water extract (LE) and to evaluate the antimicrobial activity of both LE and AgNPs.

Methods: The synthesized AgNPs were characterized using the following techniques: ultraviolet-visible spectroscopy (UV-vis), Fourier transform infrared spectroscopy (FT-IR), transmission electron microscopy (TEM), thermal gravimetric analysis (TGA), X-ray diffraction (XRD) analysis, and analysis of particle size (PS) and zeta potential (ZP). The antimicrobial activities of LE and NPs were assessed by Kirby-Bauer disc diffusion (DD) and broth microdilution (MD) methods according to the recommendations of the Clinical and Laboratory Standards Institute (CLSI). LE and AgNPs were examined against fresh cultures of four Gram-positive and five Gram-negative bacteria, and three yeast strains.

Results: AgNPs were successfully synthesized and characterized using *Arbutus andrachne* LE. The AgNPs showed moderate antibacterial activity against *Staphylococcus aureus* ATCC 6538p, *S. epidermidis* ATCC 12228, *Escherichia coli* ATCC 29998, *Klebsiella pneumoniae* ATCC 13883 and *Pseudomonas aeruginosa* ATCC 27853, and also antifungal activity against *Candida albicans* ATCC 10239 and *C. krusei* ATCC 6258.

Conclusions: Due to the potent activity of AgNPs against Gram-positive and Gram-negative bacteria, and yeast strains, it is suggested that AgNPs are potential broad spectrum antimicrobial agents.

Keywords: *Arbutus andrachne*, Silver nanoparticles, Antimicrobial activity

Tropical Journal of Pharmaceutical Research is indexed by Science Citation Index (SciSearch), Scopus, International Pharmaceutical Abstract, Chemical Abstracts, Embase, Index Copernicus, EBSCO, African Index Medicus, JournalSeek, Journal Citation Reports/Science Edition, Directory of Open Access Journals (DOAJ), African Journal Online, Bioline International, Open-J-Gate and Pharmacy Abstracts

INTRODUCTION

Nanotechnology is attracting growing interest due to its application in various fields such as medicine, biotechnology and energy consumption [1]. Nanoparticle synthesis is often used in applications such as pyrolysis, laser ablation, vapor deposition, sol gel and lithography electro-deposition [2]. Green nanoparticle synthesis from plant extracts is easy, relevant, efficient and fast compared to chemical and physical methods [3]. The

synthesis of nanoparticles by biological methods using microorganisms or plant extracts has been suggested as an eco-friendly alternative [4].

Gold nanoparticles – and silver nanoparticles (AgNPs) – are of particular interest in biology, chemistry and physics due to their optical, mechanical and electronic properties [5,6]. Silver is the most important metal in the synthesis of bionanoparticles because it is an antimicrobial agent that protects against the increasing threat posed by antibiotic resistant microbes [7].

A. andrachne (Ericaceae) is a small, evergreen tree widely found in the Mediterranean [8,9]. The leaves of *A. andrachne* contain arbutin, stilbericoside, unedosome, monotropein, catechin and epicatechin [10]. In Turkish folk medicine, the leaves are used as a diuretic, or as an astringent, or as a treatment for diarrhea and hemorrhoids [11]. The leaves of the plant have some clinical uses in arthritis, eczema, gout, rheumatism and urinary system disorders [10]. The green synthesis and characterization of AgNPs, using extracts from the *Arbutus unedo* leaf collected from Macedonia, Greece were previously reported [12].

The objective of the present study was to synthesize AgNPs using the aqueous extract of *Arbutus andrachne* leaves, to characterize these bionanoparticles and to evaluate their antimicrobial potential.

EXPERIMENTAL

Plant material

A. andrachne (Ericaceae) was collected from Cicekliköy (Izmir) during January 2012. The leaves of the plant were identified at Ege University Faculty of Pharmacy, Department of Pharmacognosy, Izmir, Turkey and a voucher specimen (no. 1266) was deposited in the Herbarium of the Faculty of Pharmacy.

Preparation of the plant extract

Dried leaf powder (5 g) was mixed with 100 mL of deionized water in an Erlenmeyer flask, and boiled for 5 min. The mixture was cooled and filtered through Whatman No.1 filter paper. The filtrate was refrigerated (10 °C) and used for further experimental procedures.

Synthesis of silver nanoparticles (AgNPs)

Silver nitrate (Sigma-Aldrich, St Louis, MO, USA) was used for the synthesis of AgNPs. For the reduction of silver ions, 10 mL of *Arbutus andrachne* leaf extract (LE) was added to 100 mL of 1 mM aqueous solution of AgNO₃ with constant stirring at 60 °C for 30 min. As soon as the extract of the leaves of *Arbutus andrachne* were mixed in an aqueous solution of the silver ion complex it started to change color from yellow to gray-brown due to excitation of the surface plasmon resonance (SPR), which indicates the formation of AgNPs. The AgNP solution obtained was purified by repeated centrifugation at 5,000 rpm for 30 min. The

solution was stored in the freeze drying flask under a vacuum below 100 Pascals at 50 °C.

Evaluation of AgNPs

Ultraviolet-visible (UV-vis) and Fourier transform infrared (FT-IR) spectroscopy analyses

UV-vis spectra were recorded as a function of reaction time on an ultraviolet-visible (UV-vis) spectrophotometer (Evolution Array; Thermo Scientific, Waltham, MA, USA) in the range of 200–800 nm at room temperature. The analyses were performed in quartz cuvettes, using distilled water as a reference. The reaction mixture was monitored spectrophotometrically at 30 min intervals from 0 to 150 min.

The functional groups of the AgNPs were characterized by a Spectrum 100 FT-IR Spectrometer (Perkin Elmer Inc., Wellesley, MA, USA) in the range of 4,000–280 cm⁻¹.

Transmission electron microscopy (TEM)

A thin film of the *A. andrachne* nanoparticles was prepared on a carbon-coated copper grid and dried under a lamp. The morphology of the AgNPs was examined by a Libra 120 transmission electron microscope (Carl Zeiss, Oberkochen, Germany).

Particle size and zeta potential measurement

For the determination of the mean particle size (PS) and the polydispersity index (PI), the formulations were evaluated within the 0.6 nm – 6 µm particle size range, at room temperature, with 137° angle using a Nano-ZS Zetasizer (Zetasizer-Nano ZS; Malvern Instruments Ltd, Malvern, UK). Three attempts were made from each sample and each trial was evaluated three times. The samples were diluted with distilled water (1:4) before evaluation.

The viscosity of the water was taken as 0.0089 poise and its refractive index was taken as 1.333. For the determination of the zeta potential (ZP), the selected formulations were evaluated at 25 °C, at an angle of 17° and 78.5 dielectric constant, 0.4 cm electrode interval, under an electrical field of 15 V/cm using a Nano-ZS Zetasizer. The samples were diluted with distilled water (1:4) before evaluation.

Thermogravimetric analysis (TGA)

Thermogravimetric analyses (TGA) were carried out with a heating rate of 20 °C/min using a

Perkin Elmer TGA-4000 thermal analyzer. The AgNPs were heated from 25 °C to a highly thermal temperature of 500 °C.

X-ray diffraction analysis (XRD)

Powder sample (AgNP) was used, and the X-ray diffraction (XRD) pattern was determined using the Rigaku Ultima IV X-ray diffractometer (Rigaku Corp., Tokyo, Japan) operated at 40 kV with a current of 20 mA using Cu-K α /radiation (λ = 1.5418 Å). The diffracted intensities were recorded from 3° to 50° 2 θ angles at a scan rate of 0.5 degree/min.

Antimicrobial activity

Antimicrobial activities of the LE and NPs were tested by the Kirby Bauer disc diffusion method and broth microdilution tests according to the recommendations of the Clinical and Laboratory Standards Institute (CLSI) against the standard test microorganisms [13-16].

Test microorganisms

Fresh cultures of nine bacteria strains (*Bacillus cereus* American Type Culture Collection (ATCC) 7064, *Staphylococcus aureus* ATCC 6538-p, *Staphylococcus epidermidis* ATCC 12228, *Streptococcus faecalis* ATCC 29212, *Escherichia coli* ATCC 29998, *Klebsiella pneumoniae* ATCC 13883, *Pseudomonas aeruginosa* ATCC 27853, *Salmonella typhimurium* CCM 5445, and *S. enterica* ATCC 13311) and three yeast strains (*Candida albicans* ATCC 10239, *C. krusei* ATCC 6258 and *C. parapsilosis* ATCC 22019) were used for the antimicrobial tests.

Disc diffusion assay

The bacteria and yeast strains were adjusted to 0.5 McFarland standard turbidity (10^{7-8} colony-forming units (CFU)/mL), and inoculated on Mueller Hinton (MH) agar with 2 % glucose and 0.5 μ g/mL methylene blue agar, respectively. The samples (10 mg/mL) were prepared in 20 % dimethyl sulphoxide (DMSO) and soaked in 6 mm sterile paper discs (BBL Microbiological Systems, Cockeysville, MD, USA) to obtain 150 μ g extract/disc concentration, and placed into inoculated agar plates. After incubation at 35 °C for 24–48 h, the diameter of the zone was recorded in millimeters (mm). All tests were performed under sterile conditions in duplicate and repeated twice. Ampicillin (Oxoid, 10 μ g/disc), ciprofloxacin (Oxoid, 5 μ g/disc) and fluconazole discs (Oxoid, 25 μ g/mL) were used as positive controls.

Microdilution method

The suspensions of the test organisms were adjusted to a 0.5 McFarland standard and 100 fold (v/v) dilutions were prepared. A dilution series of the samples was formed from 2,048 to 4 μ g/mL using Mueller Hinton (MH) broth for the bacteria and synthetic Roswell Park Memorial Institute (RPMI) 1640 medium (Sigma-Aldrich) with MOPS (Sigma-Aldrich) for the yeast strains in 96-well microtiter plates. Final concentrations in the medium were 1,024 to 2 μ g/mL, when the suspensions of the microorganisms were added to the plates. Microtiter plates were incubated at 35 °C for 24–48 h. All tests were performed under sterile conditions in duplicate and repeated twice. The 'minimum inhibitory concentration' (MIC) is defined as the lowest concentration of an antimicrobial agent that can inhibit the visible growth of a microorganism after incubation.

Standard antibacterial (ampicillin, ciprofloxacin) and antifungal (fluconazole) agents (Sigma Aldrich) were also used in the microdilution tests to maximize the accuracy of the results.

Data analysis

Three analytical replicates were performed on each sample. The results of the antimicrobial activity were analyzed and measured using one-way ANOVA. The results were averaged, and results are given as means \pm standard deviation (calculated using the Microsoft Excel software [Microsoft Corp., Redmond, WA, USA]).

RESULTS

The color of the bionanoparticles prepared by silver nitrate and LE (AgNO₃/A. *andrachne* extract) changed from yellow to gray-brown after incubation for 30 min at 50 °C. The color change was due to the collective oscillation of the free conduction electrons induced by an interacting electromagnetic field [17]. Similar changes in color have been observed in previous studies [18-19] thus confirming the completion of the reaction between the LE and AgNO₃. A. *andrachne* extract without AgNO₃ and AgNO₃ solution did not show any color changes.

A reduction of the aqueous Ag⁺ ions during exposure to the broth of boiled A. *andrachne* leaves may be easily followed by UV-vis spectroscopy (Figure 1). The UV-vis spectrum exhibited an absorption band at around 444 nm, which is a characteristic band for Ag. After 30, 60, 90, 120 and 150 min, no further change in the SPR bands were detected. This condition

indicated the completion of the reaction. The color variations were based on the excitation of the SPR resonance from the metal nanoparticles. The reduction process, Ag^+ to Ag^0 , of the nanoparticles was followed by the color change of the solution from yellow to gray-brown.

Fourier transform infrared (FT-IR) spectroscopy was performed to identify the possible biomolecules responsible for the capping and the reducing agent for the AgNPs synthesized using the *A. andrachne* water extract. *A. andrachne*

AgNPs peaks were observed at $3,202\text{ cm}^{-1}$, $1,976\text{ cm}^{-1}$, $1,691\text{ cm}^{-1}$, $1,606\text{ cm}^{-1}$, $1,297\text{ cm}^{-1}$, $1,234\text{ cm}^{-1}$, $1,015\text{ cm}^{-1}$ and 799 cm^{-1} (Figure 2).

Transmission electron microscopy (TEM) has been employed to characterize the size, shape and morphology of the synthesized AgNPs. The TEM image of the silver nanoparticles is shown in Figure 3. From the image, it is evident that the morphology of the silver nanoparticles was predominantly spherical.

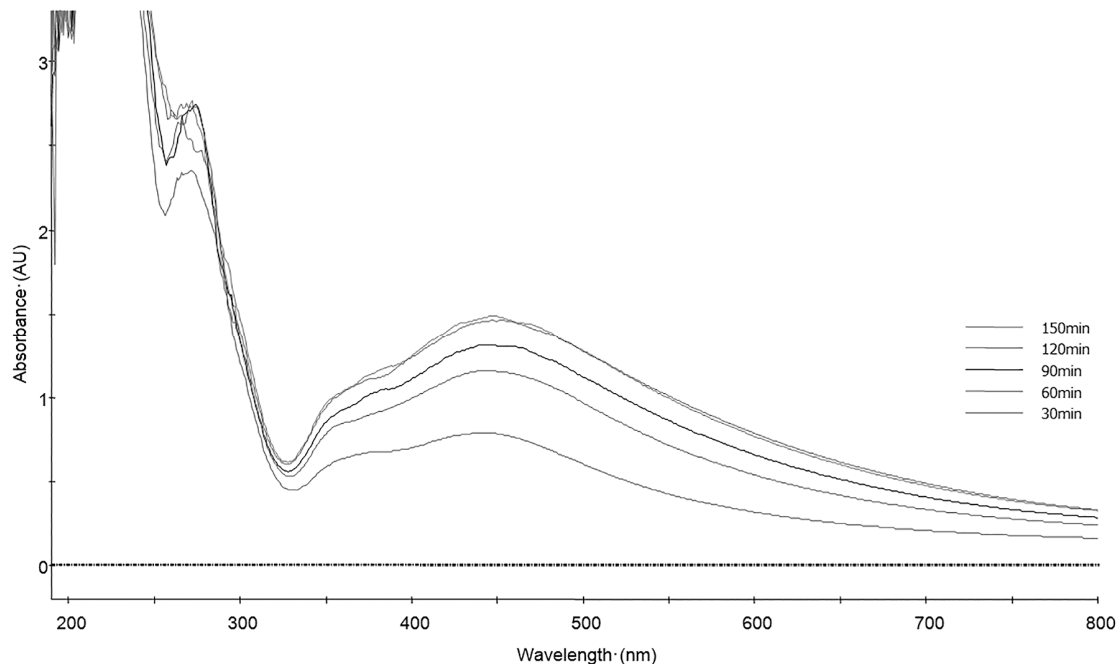


Figure 1: Ultraviolet-visible spectroscopy (UV-vis) spectra of the silver nanoparticles (AgNPs) recorded as reaction times

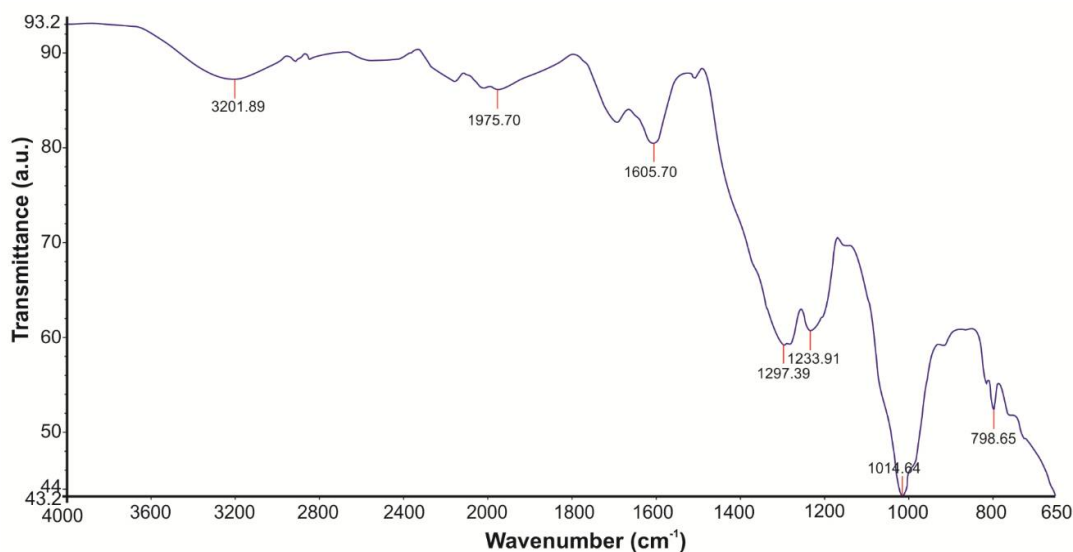


Figure 2: Fourier transform infrared (FT-IR) spectrum of AgNPs

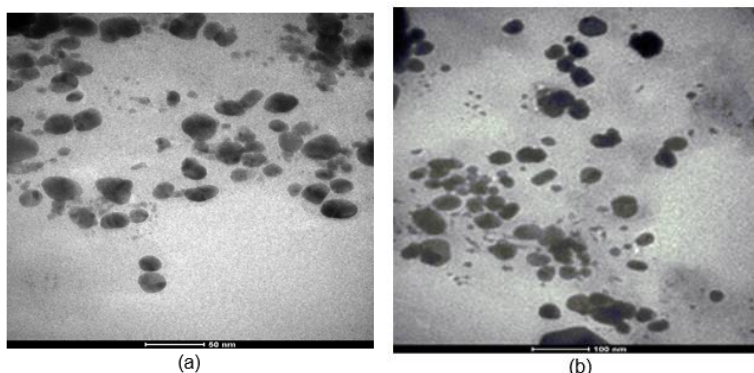


Figure 3: Transmission electron microscopy (TEM) images of AgNPs. **Note:** (a) bar = 50 nm; (b) bar = 100 nm

Particle size (PS), zeta potential (ZP) and polydispersity index (PI) values of the AgNPs are given in Table 1 and Figure 4. The mean particle size was 107.8 ± 0.8 nm.

The thermal stability of the synthesized AgNPs was monitored by TGA analysis. The weight loss

of the nanopowder due to desorption of the bioorganic compounds in the AgNPs was 28.3 %.

XRD patterns of the silver particles synthesized by *A. andrachne* water extract are shown in Figure 5.

Table 1: Particle size (PS), zeta potential (ZP) and polydispersity index (PI) values of the AgNPs (n = 3)

Formulation	PS \pm SD (nm)	ZP \pm SD (mV)	PI \pm SD
AgNP	107.8 ± 0.8	-9.4 ± 0.4	0.3 ± 0.0

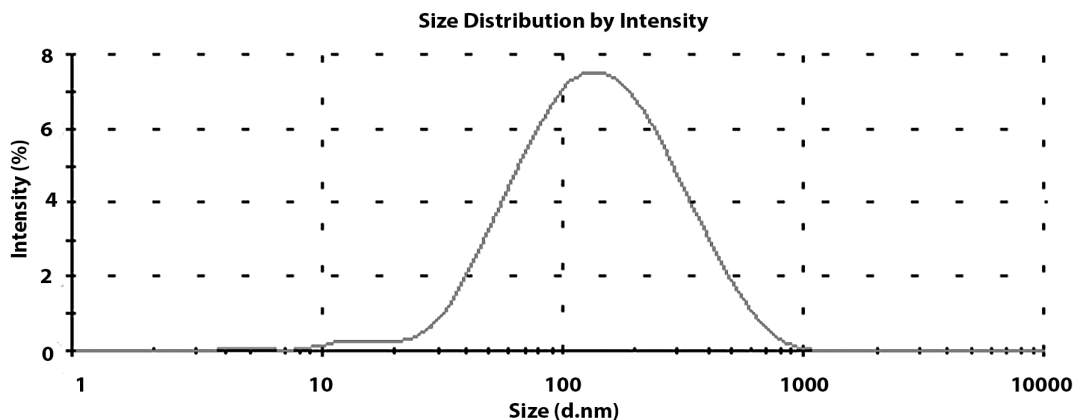


Figure 4: Particle size (PS) analysis curves for the AgNPs

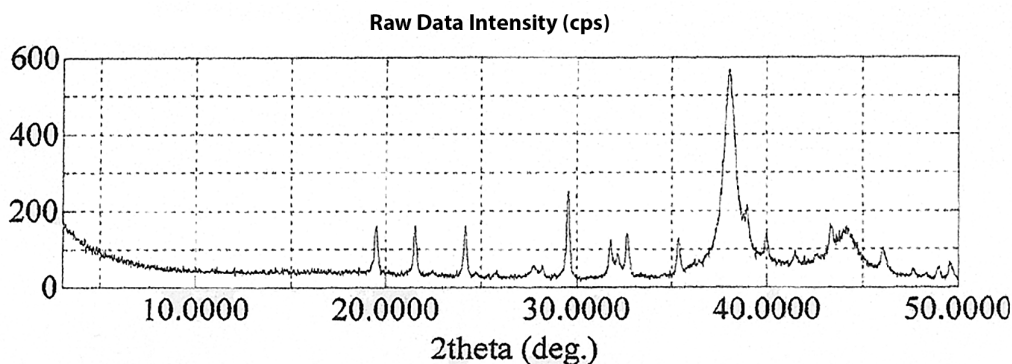


Figure 5: X-ray diffraction (XRD) patterns of the AgNPs

Table 2: Antimicrobial activity of silver nanoparticles (AgNPs) of *A. andrachne* (n = 3)

Microorganisms	Zone of inhibition \pm SD (mm)		MIC \pm SD (μ g/mL)	
	AgNPs	Amp (10 μ g/disc)	AgNP	Amp
Gram(+) bacteria				
<i>Bacillus cereus</i> ATCC 7064	8.5 \pm 0.5	17.8 \pm 0.3	5.3 \pm 2.3	6.667 \pm 2.31
<i>Staphylococcus aureus</i> ATCC 6538-p	11.0 \pm 1.0	38.0 \pm 0.5	8.0 \pm 0.0	0.833 \pm 0.29
<i>S. epidermidis</i> ATCC 12228	8.5 \pm 0.5	25.5 \pm 0.9	8.0 \pm 0.0	2.000 \pm 0.00
<i>Streptococcus faecalis</i> ATCC 29212	8.7 \pm 0.3	23.0 \pm 0.0	8.0 \pm 0.0	2.000 \pm 0.00
Gram(-) bacteria				
	AgNPs	Cip (5 μ g/disc)	AgNP	Cip
<i>Escherichia coli</i> ATCC 29998	9.5 \pm 0.5	36.8 \pm 0.3	8.0 \pm 0.0	<0.015 \pm 0.00
<i>Klebsiella pneumoniae</i> ATCC 13883	8.7 \pm 0.6	32.8 \pm 0.8	8.0 \pm 0.0	0.020 \pm 0.01
<i>Pseudomonas aeruginosa</i> ATCC 27853	10.3 \pm 0.6	33.5 \pm 0.9	8.0 \pm 0.0	0.100 \pm 0.03
<i>Salmonella typhimurium</i> CCM 5445	8.3 \pm 0.6	35.3 \pm 0.6	88.0 \pm 0.0	0.015 \pm 0.00
<i>S. enterica</i> ATCC 13311	8.5 \pm 0.5	39.3 \pm 0.6	3.3 \pm 1.2	<0.015 \pm 0.00
Yeast				
	AgNPs	Flu (25 μ g/disc)	AgNP	Flu
<i>Candida albicans</i> ATCC 10239	13.3 \pm 0.6	21.5 \pm 0.5	16.0 \pm 0.0	0.333 \pm 0.14
<i>C. krusei</i> ATCC 6258	12.2 \pm 0.8	23.7 \pm 0.6	16.0 \pm 0.0	2.667 \pm 1.15
<i>C. parapsilosis</i> ATCC 22019	12.3 \pm 0.6	22.8 \pm 0.3	5.3 \pm 2.3	4.000 \pm 0.00

AgNPs, silver nanoparticles (150 μ g/disc); Amp: Ampicillin; Cip: Ciprofloxacin; Flu: Fluconazole

The antimicrobial activity of the aqueous extract and AgNPs of *A. andrachne* were investigated qualitatively and quantitatively against the test microorganisms by determining the inhibition zones on agar plates and MIC values on micro plates. The water extract did not inhibit any of the test microorganisms. As shown in Table 2, the AgNPs had a moderate effect on the microorganisms when considering the standard antibacterial and antifungal agents. In fact, there were no huge differences in the inhibition zones and MIC values against the different organisms. According to the disc diffusion method, AgNPs were shown to be more effective against the yeast strains than the bacteria strains whereas in the microdilution test, *C. parapsilosis* ATCC 22019, *B. cereus* ATCC 7064 and *S. enterica* ATCC 13311 were found to be more susceptible to the AgNPs than the other organisms.

DISCUSSION

Green synthesized NPs can be applied in many fields such as cosmetics, foods and medicine. It has been demonstrated that the LE of *A. andrachne* is capable of producing AgNPs that are quite stable in solution. The synthesis of the AgNPs was detectable following a color change from yellow to gray-brown in the reaction solution from the incubation (UV-vis spectra), and a distinct peak was observed at 444 nm. The AgNPs exhibited a dark reddish-brown color in aqueous solution due to the SPR phenomenon [22].

Kouvaris *et al* synthesized AgNPs by using *A. andrachne* leaves and observed a sharp band of silver colloids at 436 nm [12]. Similarly, in the present study, AgNPs were synthesized using the LE of *A. andrachne* and a sharp band of silver colloids was detected at 444 nm.

The FT-IR spectrum of the synthesized nanoparticles shows bands at 3,202 cm^{-1} and 1,606 cm^{-1} , which are attributed to the O-H stretching vibrations of the phenol group and the C-H stretching of the aromatic compound, respectively. The vibration stretch in the aromatic ring confirms the presence of the aromatic group. The bands at 1,297 cm^{-1} and 1,234 cm^{-1} represent the C-O-C stretch bands. The strong peak at 1,015 cm^{-1} , which is absent for the AgNP FT-IR spectra, is the banding vibration of the C-O stretching, which could be due to stabilization of the AgNPs by this group. The C-O stretching mode in the amine group indicates the presence of proteins in the synthesized AgNPs [8]. Notably, the absorption bands at 1,976 cm^{-1} and 801 cm^{-1} in the AgNP spectrum indicated the binding of the AgNPs with oxygen from the hydroxyl groups in *A. andrachne*. Moreover, the FT-IR data revealed the presence of freely water-soluble compounds in this plant.

From the TEM images it is evident that the AgNPs are spherical, which is in agreement with the results from the SPR band in the UV-vis spectrum. The average particles size calculated on TEM was 107.8 \pm 0.8 nm, which is in good agreement with the particle size calculated by XRD analysis.

Recently, the antimicrobial properties of plant material-oriented AgNPs have been investigated in many studies. Reddy *et al* suggested that AgNPs were more effective against pathogenic bacteria than *Piper longum* fruit extract alone [20]. In this study, while the water extract of *A. andrachne* was found to be ineffective as an antimicrobial therapy, AgNPs showed moderate activity against the test organisms. The AgNPs biosynthesized using *A. andrachne* showed similar activity on all of the tested microorganisms according to the disc diffusion and the micro dilution methods. Although there are numerous studies investigating the antimicrobial effects of AgNPs, the mechanism of action is not completely understood. Some researchers have asserted that there is a relationship between their antimicrobial features and capacity to penetrate into and accumulate in the bacterial cell wall. In addition, because smaller AgNPs provided larger surfaces for the interaction with the cell wall, they exerted more inhibition on the microbial cells [21-23].

Further studies on the antimicrobial activities of AgNPs have reported various susceptibility rates for gram-negative and gram-positive bacteria and yeasts. El-Chagby and Ahmad demonstrated similar antibacterial features in AgNPs biosynthesized using *Pistacia lentiscus* leaf extract on both gram-positive and gram-negative bacteria [23]. Martinez-Gutierrez *et al* reported that there were no significant differences in the MIC results of the AgNPs against gram-positive and gram-negative bacteria. They attributed the variations among the antimicrobial activities in other studies to methodological differences [21]. In particular, gram-negative bacteria, especially *E. coli*, have been shown to be more susceptible to AgNPs compared to other tested microorganisms [22]. AgNPs show improved binding to gram-negative cell walls due to their negative charge. Owing to the thickness of the peptidoglycan layer in the cell wall structure, which protects against toxins and chemicals, gram-positive bacteria are generally found to be more resistant to antimicrobials than gram-negatives. For this reason, the efficacy of AgNPs on both gram-negative and gram-positive bacteria, as well as yeasts, might be explained by different antimicrobial mechanisms [21-23].

CONCLUSION

Biosynthesis and characterization of AgNPs from the aqueous extract of the leaves of *Arbutus andrachne* have been achieved. The antimicrobial activity of AgNPs indicate a highly inhibitory effect on Gram-positive and Gram-

negative bacteria, as well as on yeasts. The AgNPs possess potentials as therapeutic agents against pathogens and as well as for drug delivery.

ACKNOWLEDGEMENT

The authors would like to thank to Ege University Faculty of Pharmacy, Pharmaceutical Sciences Research Centre (FABAL, Izmir, Turkey).

DECLARATIONS

Conflict of Interest

No conflict of interest associated with this work.

Contribution of Authors

The authors declare that this work was done by the authors named in this article and all liabilities pertaining to claims relating to the content of this article will be borne by them.

REFERENCES

1. Bae D, Kim E, Bang J, Kim S, Han K, Lee J, Kim B, Adair J. Synthesis and characterization of silver nanoparticles by a reverse micelle process. *Met Mater Int* 2005; 4: 291-294.
2. Park HH, Choi YJ. Direct patterning of SnO(2) composite films prepared with various contents of Pt nanoparticles by photochemical metal-organic deposition. *Thin Solid Films* 2011; 519: 6214-6218.
3. Rivas L, Sanchez-Cortes S, Garcia-Ramos JV, Morcillo G. Growth of silver colloidal particles obtained by citrate reduction to increase the Raman enhancement factor. *Langmuir* 2001; 17(3): 574-577.
4. Hubenthal F. Noble metal nanoparticles: synthesis and optical properties. In: Andrews DL, Scholes GD, Wiederrecht GP. Editors. *Comprehensive Nanoscience and Technology*. Nanomaterials Elsevier Science, 2011; pp 375-435.
5. Huang X, El-Sayed IH, Qian W, El-Sayed MA. Cancer cell imaging and photothermal therapy in the near-infrared region by using gold nanorods. *J Am Chem Soc* 2006; 128: 2115-2120.
6. Li J, Wang X, Wang C, Chen B. The enhancement effect of gold nanoparticles in drug delivery and as biomarkers of drug-resistant cancer cells. *Chem Med Chem* 2007; 2: 374-378.
7. Rai MK, Deshmukh SD, Ingle AP, Gade AK. Silver nanoparticles: The powerful nanoweapon against multidrug-resistant bacteria. *J Appl Microbiol* 2012; 112: 841-852.
8. Panaek A, Kvitek A, Prucek M, Kolar M, Veerova R, Pizurova N, Sharma VK, Nevena T, Zboril R. Silver colloid nanoparticles: synthesis, characterization, and

- their antibacterial activity. *J Phys Chem* 2006; 110: 16248-16253.
9. Polunin O, Huxley A. *Flowers of the Mediterranean*, Publications of Chatto and Windows Ltd., London, 1972.
 10. Baytop, T. *Therapy with medicinal plants in Turkey (Past and present)*, Publications of the Istanbul University, Istanbul, 1984.
 11. Sakar MK, Berkman MZ, Calis I, Ruedi P. Constituents of *Arbutus andrachne*. *Fitoterapia* 1991; 62(2): 176-177.
 12. Kouvaris P, Delimitis A, Zaspalis V, Papadopoulos D, Tsipas SA, Michalidis N. Green synthesis and characterization of silver nanoparticles produced using *Arbutus unedo* leaf extract. *Materials Letters* 2012; 76: 18-20.
 13. Clinical and Laboratory Standards Institute. *Reference method for broth dilution antifungal susceptibility testing of yeasts; Approved standard, 3rd ed, CLSI document M27-A3*, Clinical and Laboratory Standards Institute, Wayne, PA 2008.
 14. Clinical and Laboratory Standards Institute. *Method for antifungal disk diffusion susceptibility testing of yeasts; Approved guideline. M44-A*, Clinical and Laboratory Standards Institute, Wayne, PA 2004.
 15. Clinical and Laboratory Standards Institute. *Methods for dilution antimicrobial susceptibility tests for bacteria that grow aerobically; approved standard-eighth edition. M07-A8*. Clinical and Laboratory Standards Institute, Wayne, PA 2009
 16. Clinical and Laboratory Standards Institute. (2009). "Performance standards for antimicrobial disk susceptibility tests; approved standard-tenth edition M02-A10. Clinical and Laboratory Standards Institute, Wayne, PA 2009
 17. Mulvaney P. *Surface Plasmon Spectroscopy of Nanosized Metal Particles*. *Langmuir* 1996; 12: 788-800.
 18. Singhal G, Bhavesh R, Kasariya K, Sharma AR, Singh RP. Biosynthesis of silver nanoparticles using *Ocimum sanctum* leaf extract and screening its antimicrobial activity. *J Nanoparticle Res.* 2011; 13: 2981-2988.
 19. Namratha N, Movica PV. Synthesis of silver nanoparticles using *Azadirachta indica* extract and usage in water purification. *Asian J Pharm Tech* 2013; 2: 228-235.
 20. Reddy NJ, Vali DN, Rani M, Edwards V, Curley M. Evaluation of antioxidant, antibacterial and cytotoxic effects of green synthesized silver nanoparticles by *Piper longum* fruit. *Material Sci and Eng C.* 2014; 34: 115-122.
 21. Martínez-Gutierrez F, Thi EP, Silverman JM, Oliveira CC, Svensson SL, Vanden Hoek A, Sanchez EM, Reiner NE, Gaegnor EC, Prydzial EL. Antibacterial activity, inflammatory response, coagulation and cytotoxicity effects of silver nanoparticles. *Nanomedicine* 2012; 8(3): 328-336.
 22. Okafor F, Janen A, Kukhtareva T, Edwards V, Curley M. Green synthesis of silver nanoparticles, their characterization, application and antibacterial activity. *Int. J Environ Res Public Health* 2013; 10(10): 5221-5238.
 23. El-Chaghaby GA, Ahmad AF. Biosynthesis of silver nanoparticles using *Pistacia lentiscus* leaves extract and investigation of their antimicrobial effect. *Oriental J Chem* 2011; 27 (3): 929-936.